

1 / JAST (Journal of Animal Science and Technology) TITLE PAGE

2 Upload this completed form to website with submission

3

ARTICLE INFORMATION	Fill in information in each box below
Article Type	Research article
Article Title (within 20 words without abbreviations)	Lauric acid reduces apoptosis by inhibiting FOXO3a-signaling in Deoxynivalenol-treated IPEC-J2 cells
Running Title (within 10 words)	Lauric acid alleviates DON-induced damage in IPEC-J2 cells.
Author	Na Yeon Kim ¹ , Sang In Lee ¹
Affiliation	Department of Animal Biotechnology, Kyungpook National University, Sangju, Gyeongsangbuk-do 37224, Republic of Korea
ORCID (for more information, please visit https://orcid.org)	Not applicable
Competing interests	No potential conflict of interest relevant to this article was reported.
Funding sources State funding sources (grants, funding sources, equipment, and supplies). Include name and number of grant if available.	Not applicable.
Acknowledgements	This research was supported by the Basic Science Research Program through the National Research Foundation of Korea (NRF) funded by the Ministry of Education (2022R111A3070740).
Availability of data and material	Upon reasonable request, the datasets of this study can be available from the corresponding author.
Authors' contributions Please specify the authors' role using this form.	Conceptualization: Lee SI. Data curation: Kin NY, Lee SI Formal analysis: Kin NY, Lee SI Methodology: Kin NY, Lee SI Validation: Kin NY, Lee SI Writing - original draft: Kin NY, Lee SI
Ethics approval and consent to participate	This article does not require IRB/IACUC approval because there are no human and animal participants.

4

5 CORRESPONDING AUTHOR CONTACT INFORMATION

For the corresponding author (responsible for correspondence, proofreading, and reprints)	Fill in information in each box below
First name, middle initial, last name	Sang In Lee
Email address – this is where your proofs will be sent	silee78@knu.ac.kr
Secondary Email address	
Address	2559 Gyeongsang-daero, Sangju-si, Gyeongsangbuk-do, Republic of Korea (37224)
Cell phone number	82-10-4183-5813
Office phone number	82-54-530-1943
Fax number	82-54-530-1949

6

7

Abstract

8

9 Deoxynivalenol (DON) is the most common mycotoxin contaminant of food or feed worldwide and
10 causes disease in animals. Lauric acid (LA) is a medium-chain fatty acid useful for barrier functions
11 such as antimicrobial activity in the intestine of monogastric animals. However, the molecular
12 mechanisms by which lauric acid exerts its effects on the deoxynivalenol-exposed small intestine have
13 not been studied. We used an intestinal porcine epithelial cell line (IPEC-J2) as an *in vitro* model to
14 explore the molecular mechanism of lauric acid in alleviating deoxynivalenol-induced damage. We
15 found that lauric acid reversed deoxynivalenol-induced reduction in cell viability. Our qRT-PCR results
16 indicated that lauric acid alleviated deoxynivalenol-induced apoptosis through Annexin-V. Additionally,
17 immunofluorescence and Western blotting showed that lauric acid attenuated deoxynivalenol-induced
18 Forkhead box O3 (FOXO3a) translocation. These results suggest that lauric acid attenuates Forkhead
19 box O3 translocation in the small intestine damaged by deoxynivalenol, thereby reducing apoptosis. In
20 conclusion, this study found that lauric acid alleviates deoxynivalenol-induced damage in intestinal
21 porcine epithelial cell line through various molecular mechanisms.

22 **Keywords:** IPEC-J2 cells, Deoxynivalenol, Lauric acid, Apoptosis, Foxo3a

23

Introduction

24

25 The intestinal epithelium digests and absorbs nutrients and forms a barrier against pathogens and toxic
26 substances [1, 2]. The intestinal epithelium is also important for maintaining health as it is the first
27 physical barrier to detect external substances [3]. Damage to the intestinal epithelium disrupts immune
28 homeostasis, increases inflammation, disrupts its function as a barrier and leads to many intestinal
29 diseases, including pathogenic infections [4, 5]. The intestinal epithelium is constantly exposed to
30 bacteria, fungi, viruses, and parasites that can act as pathogens [6]. The intestinal epithelium is exposed
31 to higher concentrations of mycotoxins than other organs, thus, it is the first to suffer toxic damage [7,
32 8]. Exposure of the intestinal epithelium to mycotoxins disrupts its function as a barrier through
33 disrupted intestinal integrity (physical), thinned mucus layer (chemical), imbalanced inflammatory
34 factors (immunological), and dysfunctional bacterial homeostasis (microbial) [8].

35 DON is a mycotoxin produced by *Fusarium* species and contaminates food and feed worldwide [9].
36 DON mainly contaminates crops such as maize, wheat, and barley and exposure to it poses a health
37 threat to both humans and animals [10]. Pigs are the most susceptible animals to DON [11]. After eating
38 DON-contaminated feed, they suffer from anorexia, vomiting, diarrhea, and deterioration of their
39 immune and reproductive functions [12]. Additionally, DON affects growth and weight gain rate, and
40 causes stiff pig syndrome, abortion, stillbirth, and weak offspring [13]. Current methods to reduce
41 exposure to mycotoxins include thermal processing, chemical agents, and toxin binders [14]. However,
42 these methods do not completely destroy mycotoxins, and toxin binders change their nutritional value
43 and reduce bioavailability of trace minerals or vitamins [15]. Therefore, research on other natural
44 products that can alleviate mycotoxins is required.

45 LA is a medium-chain fatty acid (MCFAs) composed of 12 carbon atoms and is found in coconut oil,
46 milk, and black soldier flies (BSF, *Hermetia illucens* L.) [16, 17]. MCFAs, including LA, influence
47 nutritional functions, digestion, absorption, and energy supply in monogastric intestines, while also
48 regulating immune responses, relieving stimulus-induced symptoms, and contributing to barrier
49 functions [18-20]. Therefore, LA, one of MCFAs, can be used as an inexpensive and new feed additive

50 to replace antibiotics [20, 21]. Nevertheless, the molecular mechanisms by which LA benefit the
51 mycotoxin-damaged small intestine epithelium are unknown and require further study. Therefore, in
52 this study, we investigated the molecular mechanism of LA on DON-induced dysfunction in porcine
53 small intestinal epithelium using IPEC-J2 cells.

54

55

Materials and Methods

56

Cell Culture and Treatment

57 IPEC-J2 cells (DSMZ, Braunschweig, Germany) isolated from unsuckling piglet jejunal epithelium
58 were cultured in Dulbecco's Modified Eagle Medium (Thermo Fisher Scientific, Wilmington, DE, USA)
59 supplemented with 10% fetal bovine serum and 1% penicillin-streptomycin in a 37°C CO₂ incubator.
60 Lauric acid (Sigma–Aldrich, St. Louis, MO, USA) was diluted with dimethyl sulfoxide for treating
61 IPEC-J2 cells.
62

63

Cell viability

64 IPEC-J2 cells were seeded in 3×10^4 cells in a 96-well plate, cultured for 24 h, before they were exposed
65 to LA (0, 0.1, 0.2, 0.3, 0.4, and 0.5 mM) or LA(0.2 mM) and DON (0.25 ug) for 24 h. After 2 h of
66 treatment with Water-Soluble Tetrazolium 1 (WST-1)(Roche Diagnostics GmbH, Mannheim, Germany),
67 cell viability was measured by analyzing the absorbance of the dye by subtracting the background
68 wavelength from 450 nm to 600 nm using a GloMax Discover Multi-Microplate Reader. And Cell
69 viability was compared to control group and was calculated by converting absorbance to percentage.
70

71

Annexin-V and propidium iodide stainings

72 After 24 h of LA and DON treatment, IPEC-J2 cells were harvested, washed with PBS, and centrifuged.
73 After discarding the supernatant, $1 \times$ Annexin binding buffer $5 \mu\text{L}$ Alexa Fluor 488 Annexin-V (Thermo
74 Fisher Scientific, Wilmington, DE, USA), and $1 \mu\text{L}$ 100 mg/mL PI working solution were added. After
75

76 incubation of the cells at room temperature for 15 min in the dark, the nucleus was stained with DAPI
77 (Vector Laboratories, Burlingame, CA, USA) and mounted on a slide using a coverslip. Pictures of the
78 cells were taken using a fluorescence microscope (Korealabtech, Seongnam-si, Gyeonggi-do, Korea).

79

80 Immunofluorescence staining of cells

81 IPEC-J2 cells treated with LA and DON were grown on gelatin-coated glass cover slips for 24 h before
82 they were fixed with 4% paraformaldehyde for 15 min. After that, the cells were treated with a blocking
83 buffer for 1 h. Rabbit anti-FOXO3a IgG was treated with a 1:200 antibody solution and probed
84 overnight. After washing with PBS three times for 3 min, goat antirabbit (488) (Thermo Fisher
85 Scientific, Carlsbad, CA, USA) was treated with the antibody solution at a ratio of 1:500 and incubated
86 for 1 h in the dark. Thereafter, the nucleus was stained with DAPI (Vector Laboratories, Burlingame,
87 CA, USA) covered with a cover slip, the cells were photographed under a fluorescence microscope.

88

89 Extraction of cytoplasmic and nuclear proteins

90 Cytoplasmic and nuclear proteins were extracted using NE-PER Nuclear and Cytoplasmic Extraction
91 Reagent (Thermo, Wilmington, DE, USA) according to the manufacturer's instructions. Cells were
92 washed with chilled PBS and centrifuged at 1200 rpm for 3 min. After discarding the supernatant,
93 cytoplasmic extraction reagent I (CERI) was added to the cell pellet, vortexed for 15 s before the
94 suspension was incubated on ice for 10 min. Cytoplasmic extraction reagent II (CERII) was added and
95 vortexing for 15 s, the mixture was incubated on ice for 1 min. After centrifugation of the suspension
96 at 14000 rpm, the cytoplasmic extraction suspension was transferred to a prechilled tube. A nuclear
97 extraction reagent (NER) was added to the insoluble pellet before vortexing for 15 s every 10 min for a
98 total of 40 min. After centrifugation at 14000 rpm for 10 min, the supernatant was transferred into a
99 prechilled tube. The extracted protein was analyzed for protein concentration using the Pierce
100 Bicinchoninic acid (BCA) Protein Assay Kit (Thermo Fisher Scientific, Waltham, MA, USA). The
101 extracted proteins were used in subsequent analyses.

102

103 Western blotting

104 Protein samples were denatured in 4X Laemmli buffer (4% sodium dodecyl sulfate, 10% 2-
105 mercaptoethanol, 20% glycerol, 0.004% bromophenol blue, and 0.125 M Tris-HCl) (3:1) at 95°C for 5
106 min. Proteins were electrophoretically separated on 12% sodium dodecyl sulfate-polyacrylamide gel
107 electrophoresis (SDS-PAGE) gels (run for 1 h at 100 V) before they were transferred to polyvinylidene
108 fluoride membranes (Thermo Fisher Scientific). After blocking for 2 h, the proteins were treated with
109 anti-FOXO3a (Novus Biologicals, Centennial, CO, USA) antibody overnight. The membrane was
110 washed three times with Tris-buffered saline containing Tween 20 (TBST, 20 mM Tris, pH 7.5, 150
111 mM NaCl and 0.1% Tween 20) for 10 min before it was treated with a secondary antibody for 1 h at
112 room temperature. Protein bands were visualized for immunoreactivity using the Enhanced
113 Chemiluminescence (ECL) reagent, and protein bands were imaged using the ChemiDoc imaging
114 system.

115

116 RT-PCR

117 Total RNA extraction was performed using the AccuPreP Universal RNA Extraction kit (BioNEER,
118 Daejeon, Korea). cDNA was synthesized from total RNA (1 µg) using the DiaStar™ RT Kit (SolGent,
119 Daejeon, Korea). Primer 3 (<http://frodo.wi.mit.edu>) was used to design primers for target genes in qPCR.
120 For qRT-PCR, 40 cycles of 95°C for 3 min, 95°C for 15 sec, 56 °C–58°C for 15 sec, and 72°C for 15 s
121 were used. Levels of target genes were calculated using the 2- $\Delta\Delta C_t$ method, normalized to
122 glyceraldehyde-3-phosphate dehydrogenase (GAPDH). The primer sequences of the genes are shown
123 in Table 1.

124

125 Statistical analysis

126 The general linear model (PROC-GLM) procedure in SAS was used to test for significant differences
127 between treatment groups. Figure1B Data were analyzed using t-tests. Symbols of significance were
128 set as **p < 0.01, ***p < 0.001. For other cell viability and PCR data were evaluated for significant
129 differences between treatment groups using Duncan's multiple range test. All experiments were

130 performed independently in triplicate.

131 **Results**

132

133 LA affects cell proliferation in IPEC-J2 cells

134 To confirm the cell viability of LA for IPEC-J2 cells, the cell proliferation analysis WST-1 assay was
135 performed. IPEC-J2 cells were exposed to LA at different concentrations (0, 0.1, 0.2, 0.3, 0.4, and 0.5
136 mM); Concentrations of 0.1–0.2 mM of LA increased cell proliferation whereas LA at concentrations
137 of 0.3 mM or higher decreased cell proliferation (Fig 1A). Therefore, LA concentration of 0.2 mM was
138 chosen for further analyses. The effect of 0.2 mM LA on IPEC-J2 cells was time dependents cell
139 proliferation increased at 24, 48, 72, and 96 h (Fig 1B). Accordingly, we used 24 h for further analyses.
140 Cell viability was compared between all treated and control groups by converting absorbance values
141 into percentages as shown in the figure.

142

143 LA affects DON-induced cell proliferation in IPEC-J2 cells

144 We used the cell proliferation analysis WST-1 assay to assess whether LA affects cell proliferation
145 capacity induced by DON. IPEC-J2 cells treated with DON showed significantly lower cell proliferation
146 than those in the control. However, we observed that when DON-treated IPEC-J2 cells were co-treated
147 with LA, cell proliferation increased (Fig 2), indicating that LA alleviates DON-induced reduction in
148 cell proliferation capacity.

149

150 LA alleviates DON-induced apoptosis and necrosis in IPEC-J2 cells

151 To determine whether LA alleviates DON-induced apoptosis and necrosis in IPEC-J2 cells, we
152 performed double staining with Annexin-V and propidium iodide. Apoptosis and necrosis were
153 significantly increased in IPEC-J2 cells treated with DON. In contrast, when IPEC-J2 cells exposed to
154 DON were treated with LA, apoptosis and necrosis were reduced (Fig 3A). Additionally, when
155 examining the mRNA expression levels of apoptosis-related genes such as Bcl-2, Bcl-6, CASP3, and
156 CASP9, the mRNA expression was significantly lower when cells were exposed to both LA and DON

157 than to DON alone. Moreover, the mRNA expression of FOXO3a was also higher in cells exposed to
158 DON than in those in the control and decreased when cells were treated with LA (Fig 3B)., indicating
159 that LA alleviates DON-induced apoptosis and necrosis.

160

161 LA attenuates DON-induced FOXO3a translocation to the nucleus

162 Annexin-V results showed that LA alleviated DON-induced apoptosis and necrosis. We hypothesized
163 that this might be influenced by FOXO3a signaling. Therefore, we measured the expression of FOXO3a
164 protein in IPEC-J2 cells using immunocytochemistry, Western blotting, and real-time PCR.
165 Immunocytochemistry results showed that DON-induced FOXO3a nuclear translocation was similar to
166 that of the control. However, DON-induced FOXO3a nuclear translocation was attenuated in cells co-
167 treated with DON and LA (Fig 4A). Additionally, Western blotting results showed that the expression
168 of FOXO3a was significantly decreased in the cytoplasm and significantly increased in the nucleus of
169 DON-treated IPEC-J2 cells. In contrast, in IPEC-J2 cells co-treated with LA and DON, the expression
170 of FOXO3a significantly increased in the cytoplasm and significantly decreased in the nucleus (Fig 4B).

171

172

Discussion

173

174 DON is a mycotoxin that causes various symptoms such as anorexia, vomiting, and stunted growth,
175 leading to poor health and economic loss [22]. The intestine is the first biological barrier to mycotoxins
176 because it is the first target of exposure after consuming contaminated food [23, 24]. Intestinal exposure
177 to DON causes symptoms such as destruction of intestinal epithelial cells, impairment of integrity of
178 intestinal barrier, destruction of tight junction protein structures, increased intestinal epithelial
179 permeability, reduced nutrient absorption and transport efficiency, inflammation, and induction of
180 apoptosis [25]. To reduce exposure to mycotoxins, various methods such as toxin binders are used, but
181 they are not completely effective [14, 15]. Lauric acid is a MCFA that promotes intestinal health through
182 its effects such as antibacterial activity, reduction of inflammatory response, and reduction of oxidative

183 stress [18, 26]. Previous studies have shown that LA has beneficial effects on the intestine through its
184 antibacterial activity [27-29]. Therefore, LA can be used as a new feed additive to replace antibiotics.
185 Thus, we speculated that LA would alleviate DON-induced damage to the small intestine epithelial cells.
186 First, we investigated the cytotoxicity of various concentrations of LA to IPEC-J2 cells. The WST-1
187 assay showed that LA concentrations of 0.1 and 0.2 mM had a beneficial effect on cell proliferation.
188 However, there was no statistically significant difference between 0.1 and 0.2 mM in cell viability.
189 Therefore, further analyses were conducted using an LA concentration of 0.2 mM. In a previous study,
190 when IPEC-J2 cells were exposed to DON at a concentration of 250 ng/mL, cell proliferation was
191 significantly lower than that of the control group [30]. Therefore, we decided to use DON at a
192 concentration of 250 ng/mL for further analyses. We observed that cell proliferation was significantly
193 higher in cells co-exposed to LA at 0.2 mM and DON than in cells exposed only to DON 0.25 ug/mL.
194 Apoptosis is a highly regulated cell death process induced by various stimuli such as mycotoxins and
195 unfavorable physiological conditions, which can damage the intestinal epithelium and lead to intestinal
196 pathology [31-33]. Reduced cell proliferation is associated with increased apoptosis [34, 35]. Therefore,
197 we speculated that cell proliferation reduced by DON and increased when treated with LA might also
198 be related to apoptosis. FOXO3a induces apoptosis by inhibiting the apoptosis-inhibitor protein [36]. It
199 also induces the expression of several proapoptotic members, including Bcl-2 and Bcl-6, to inhibit cell
200 growth and promote apoptotic signaling [33, 37]. Expression of these proapoptotic proteins catalyzes
201 the activation of the initiator caspase (caspase-9), which in turn activates the effector factor (caspase-3)
202 [38, 39]. Activated caspase-3 causes morphological changes in apoptotic cells [39]. For example,
203 caspase-3 cleavage of caspase-activated DNase (ICAD) initiates activation of caspase-activated
204 DNase (CAD). The activation of CAD then cleaves the DNA at the inter-nucleosome linker sites,
205 leading to chromatin condensation and DNA fragmentation [40, 41]. This form of DNA fragmentation
206 is a common characteristic of cells undergoing apoptosis. In addition, Bcl-2 is overexpressed to prevent
207 cell death in the early stages of necrotic activation [42]. Our RT-PCR results showed that the mRNA
208 expression of FOXO3a was increased in cells exposed to DON but decreased in those exposed LA.

209 Also, genes related to apoptosis such as Bcl-2, Bcl-6, caspase 3, and caspase 9 were increased by DON
210 and decreased by LA relative to the control group. Additionally, we observed that LA alleviated DON-
211 induced apoptosis and necrosis through Annexin-V staining. Therefore, our findings confirmed that LA
212 mitigated DON-induced apoptosis and necrosis in IPEC-J2 cells.

213 The forkhead box O (FOXO) protein activates or inhibits the transcription of target genes through its
214 DNA-binding foxo domain in the nucleus via the nucleocytoplasmic shuttle, and regulates cell cycle
215 arrest, DNA repair and apoptosis, stress, and tumor suppressor pathways [43]. FOXO family members
216 of the Forkhead transcription factor include Foxo1, Foxo3, Foxo4, and Foxo6 [44]. Among several
217 FOXO family members, FOXO3a is abundant in various tissues including the brain, heart, kidney, and
218 spleen and is the most important transcription factor involved in apoptosis and cell cycle inhibition [33,
219 43]. Upon intestinal exposure to factors such as mycotoxin, FOXO3a protein translocates from the
220 nucleocytoplasm to the nucleus to form DNA-binding foxo domains, triggering apoptosis and leading
221 to intestinal damage (Fig 5A). Our immunocytochemistry and Western blotting analysis showed that
222 DON treatment induced nuclear translocation of FOXO3a protein. In contrast, DON-induced nuclear
223 translocation of FOXO3a protein was attenuated when cells were co-treated with DON and LA (Fig
224 5B). Our results show that LA reversed the increase in apoptosis caused by DON-induced nuclear
225 translocation of the FOXO3a protein in IPEC-J2 cells.

226 This study is the first to investigate the effect of LA on DON-treated porcine intestinal epithelial cells.
227 Our findings indicated that LA alleviated DON-induced reduction in cell proliferation and DON-
228 induced increase in apoptosis (Fig 5A, B). This suggests that LA has a beneficial effect on DON-induced
229 damage to the intestinal epithelium. Additionally, our results suggest that LA can be used as a natural
230 antibiotic in the future.

231

232

References

233

234 1. Yang, H., et al., Effects of Weaning on Intestinal Upper Villus Epithelial Cells of Piglets. *PLoS One*, 2016.
235 11(3): p. e0150216.

236 2. Jang, H.J. and S.I. Lee, MicroRNA expression profiling during the suckling-to-weaning transition in pigs. *J*
237 *Anim Sci Technol*, 2021. 63(4): p. 854-863.

238 3. Kang, R., et al., Deoxynivalenol induced apoptosis and inflammation of IPEC-J2 cells by promoting ROS
239 production. *Environ Pollut*, 2019. 251: p. 689-698.

240 4. Yi, H., et al., Cathelicidin-WA Improves Intestinal Epithelial Barrier Function and Enhances Host Defense
241 against Enterohemorrhagic *Escherichia coli* O157:H7 Infection. *J Immunol*, 2017. 198(4): p. 1696-1705.

242 5. Mun, D., et al., Effects of *Bacillus*-based probiotics on growth performance, nutrient digestibility, and
243 intestinal health of weaned pigs. *J Anim Sci Technol*, 2021. 63(6): p. 1314-1327.

244 6. Gallo, R.L. and L.V. Hooper, Epithelial antimicrobial defence of the skin and intestine. *Nat Rev Immunol*,
245 2012. 12(7): p. 503-16.

246 7. Ren, Z., et al., Progress in Mycotoxins Affecting Intestinal Mucosal Barrier Function. *Int J Mol Sci*, 2019.
247 20(11).

248 8. Gao, Y., et al., The Compromised Intestinal Barrier Induced by Mycotoxins. *Toxins (Basel)*, 2020. 12(10).

249 9. Zhang, C., et al., Deoxynivalenol triggers porcine intestinal tight junction disorder: Insights from
250 mitochondrial dynamics and mitophagy. *Ecotoxicol Environ Saf*, 2022. 248: p. 114291.

251 10. Liao, S., et al., Chloroquine Improves Deoxynivalenol-Induced Inflammatory Response and Intestinal
252 Mucosal Damage in Piglets. *Oxid Med Cell Longev*, 2020. 2020: p. 9834813.

253 11. Garcia, G.R., et al., Intestinal toxicity of deoxynivalenol is limited by *Lactobacillus rhamnosus* RC007 in pig
254 jejunum explants. *Arch Toxicol*, 2018. 92(2): p. 983-993.

255 12. Wang, S., et al., Deoxynivalenol Impairs Porcine Intestinal Host Defense Peptide Expression in Weaned
256 Piglets and IPEC-J2 Cells. *Toxins (Basel)*, 2018. 10(12).

257 13. Yao, Y. and M. Long, The biological detoxification of deoxynivalenol: A review. *Food Chem Toxicol*, 2020.
258 145: p. 111649.

259 14. Colovic, R., et al., Decontamination of Mycotoxin-Contaminated Feedstuffs and Compound Feed. *Toxins*
260 *(Basel)*, 2019. 11(11).

- 261 15. Hussein, H.S. and J.M. Brasel, Toxicity, metabolism, and impact of mycotoxins on humans and animals.
262 Toxicology, 2001. 167(2): p. 101-34.
- 263 16. Yang, Y., et al., The Effects of Lauric Acid on IPEC-J2 Cell Differentiation, Proliferation, and Death. *Curr*
264 *Mol Med*, 2020. 20(7): p. 572-581.
- 265 17. Surendra, K.C., et al., Rethinking organic wastes bioconversion: Evaluating the potential of the black soldier
266 fly (*Hermetia illucens* (L.)) (Diptera: Stratiomyidae) (BSF). *Waste Manag*, 2020. 117: p. 58-80.
- 267 18. Jia, M., et al., Effects of Medium Chain Fatty Acids on Intestinal Health of Monogastric Animals. *Curr*
268 *Protein Pept Sci*, 2020. 21(8): p. 777-784.
- 269 19. Lauridsen, C., Effects of dietary fatty acids on gut health and function of pigs pre- and post-weaning. *J Anim*
270 *Sci*, 2020. 98(4).
- 271 20. Jackman, J.A., R.D. Boyd, and C.C. Elrod, Medium-chain fatty acids and monoglycerides as feed additives
272 for pig production: towards gut health improvement and feed pathogen mitigation. *J Anim Sci Biotechnol*,
273 2020. 11: p. 44.
- 274 21. Zheng, C., et al., Effects of a combination of lauric acid monoglyceride and cinnamaldehyde on growth
275 performance, gut morphology, and gut microbiota of yellow-feathered broilers. *Poult Sci*, 2023. 102(8): p.
276 102825.
- 277 22. Vandembroucke, V., et al., The mycotoxin deoxynivalenol potentiates intestinal inflammation by *Salmonella*
278 *typhimurium* in porcine ileal loops. *PLoS One*, 2011. 6(8): p. e23871.
- 279 23. Chen, J., et al., Plant-Derived Polyphenols as Nrf2 Activators to Counteract Oxidative Stress and Intestinal
280 Toxicity Induced by Deoxynivalenol in Swine: An Emerging Research Direction. *Antioxidants* (Basel), 2022.
281 11(12).
- 282 24. Yoon, J.W. and S.I. Lee, Gene expression profiling after ochratoxin A treatment in small intestinal epithelial
283 cells from pigs. *J Anim Sci Technol*, 2022. 64(5): p. 842-853.
- 284 25. Tang, M., D. Yuan, and P. Liao, Berberine improves intestinal barrier function and reduces inflammation,
285 immunosuppression, and oxidative stress by regulating the NF-kappaB/MAPK signaling pathway in
286 deoxynivalenol-challenged piglets. *Environ Pollut*, 2021. 289: p. 117865.
- 287 26. Tham, Y.Y., et al., Lauric acid alleviates insulin resistance by improving mitochondrial biogenesis in THP-1
288 macrophages. *Mol Biol Rep*, 2020. 47(12): p. 9595-9607.
- 289 27. Wu, Y., et al., Serum metabolome and gut microbiome alterations in broiler chickens supplemented with
290 lauric acid. *Poult Sci*, 2021. 100(9): p. 101315.
- 291 28. Zeng, X., et al., Dietary butyrate, lauric acid and stearic acid improve gut morphology and epithelial cell
292 turnover in weaned piglets. *Anim Nutr*, 2022. 11: p. 276-282.

- 293 29. Liu, Z.H., et al., Lauric acid alleviates deoxynivalenol-induced intestinal stem cell damage by potentiating
294 the Akt/mTORC1/S6K1 signaling axis. *Chem Biol Interact*, 2021. 348: p. 109640.
- 295 30. Wang, X., et al., Deoxynivalenol Induces Inflammatory Injury in IPEC-J2 Cells via NF-kappaB Signaling
296 Pathway. *Toxins (Basel)*, 2019. 11(12).
- 297 31. Xu, X., Y. Lai, and Z.C. Hua, Apoptosis and apoptotic body: disease message and therapeutic target potentials.
298 *Biosci Rep*, 2019. 39(1).
- 299 32. Negroni, A., S. Cucchiara, and L. Stronati, Apoptosis, Necrosis, and Necroptosis in the Gut and Intestinal
300 Homeostasis. *Mediators Inflamm*, 2015. 2015: p. 250762.
- 301 33. Kang, T.H., K.S. Kang, and S.I. Lee, Deoxynivalenol Induces Apoptosis via FOXO3a-Signaling Pathway in
302 Small-Intestinal Cells in Pig. *Toxics*, 2022. 10(9).
- 303 34. Leard, L.E. and V.C. Broaddus, Mesothelial cell proliferation and apoptosis. *Respirology*, 2004. 9(3): p. 292-
304 9.
- 305 35. Zhao, W., et al., Liraglutide inhibits the proliferation and promotes the apoptosis of MCF-7 human breast
306 cancer cells through downregulation of microRNA-27a expression. *Mol Med Rep*, 2018. 17(4): p. 5202-
307 5212.
- 308 36. Hagenbuchner, J. and M.J. Ausserlechner, Mitochondria and FOXO3: breath or die. *Front Physiol*, 2013. 4:
309 p. 147.
- 310 37. Melnik, B.C., Apoptosis May Explain the Pharmacological Mode of Action and Adverse Effects of
311 Isotretinoin, Including Teratogenicity. *Acta Derm Venereol*, 2017. 97(2): p. 173-181.
- 312 38. Brunet, A., S.R. Datta, and M.E. Greenberg, Transcription-dependent and -independent control of neuronal
313 survival by the PI3K-Akt signaling pathway. *Curr Opin Neurobiol*, 2001. 11(3): p. 297-305.
- 314 39. Eskandari, E. and C.J. Eaves, Paradoxical roles of caspase-3 in regulating cell survival, proliferation, and
315 tumorigenesis. *J Cell Biol*, 2022. 221(6).
- 316 40. Enari, M., et al., A caspase-activated DNase that degrades DNA during apoptosis, and its inhibitor ICAD.
317 *Nature*, 1998. 391(6662): p. 43-50.
- 318 41. Larsen, B.D. and C.S. Sorensen, The caspase-activated DNase: apoptosis and beyond. *FEBS J*, 2017. 284(8):
319 p. 1160-1170.
- 320 42. Nikolettou, V., et al., Crosstalk between apoptosis, necrosis and autophagy. *Biochim Biophys Acta*, 2013.
321 1833(12): p. 3448-3459.
- 322 43. Zhang, X., et al., Akt, FoxO and regulation of apoptosis. *Biochim Biophys Acta*, 2011. 1813(11): p. 1978-

323 86.

324 44. Snoeks, L., et al., Tumor suppressor Foxo3a is involved in the regulation of lipopolysaccharide-induced
325 interleukin-8 in intestinal HT-29 cells. *Infect Immun*, 2008. 76(10): p. 4677-85.

326

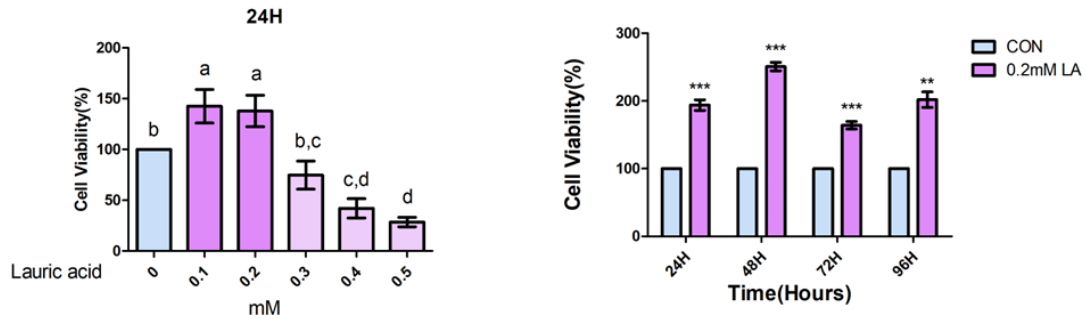
327

ACCEPTED

328

Tables and Figures

329



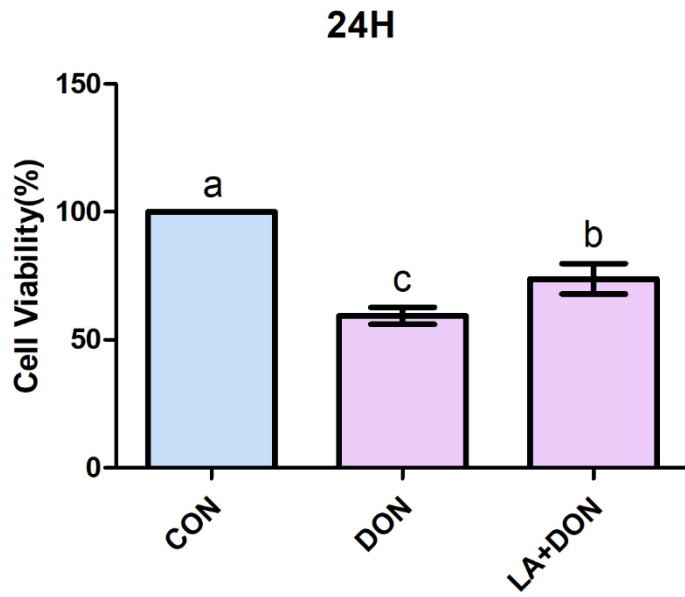
330

331 **Figure 1.** Lauric acid promotes IPEC-J2 cells proliferation at 0.1, 0.2 mM, and decreases the cell
332 viability at the concentration of 0.4 mM or higher. A. The WST-1 assay of the IPEC-J2 cells after
333 exposure to 0-0.5mM LA for 24H (n=3). Error bars indicated standard errors (SEs) of triplicate analysis.
334 Lowercase letters (a, b, c and d) mean significant differences between groups based on Duncan's multi-
335 range test. B. The WST-1 assay of IPEC-J2 cells on treatment with 0.2mM for 24h, 48h, 72h, and 96h,
336 compared to untreated control (n=3). Error bars indicated standard errors (SEs) of triplicate analysis.
337 ** $p < 0.01$, *** $p < 0.001$.

338

339

340

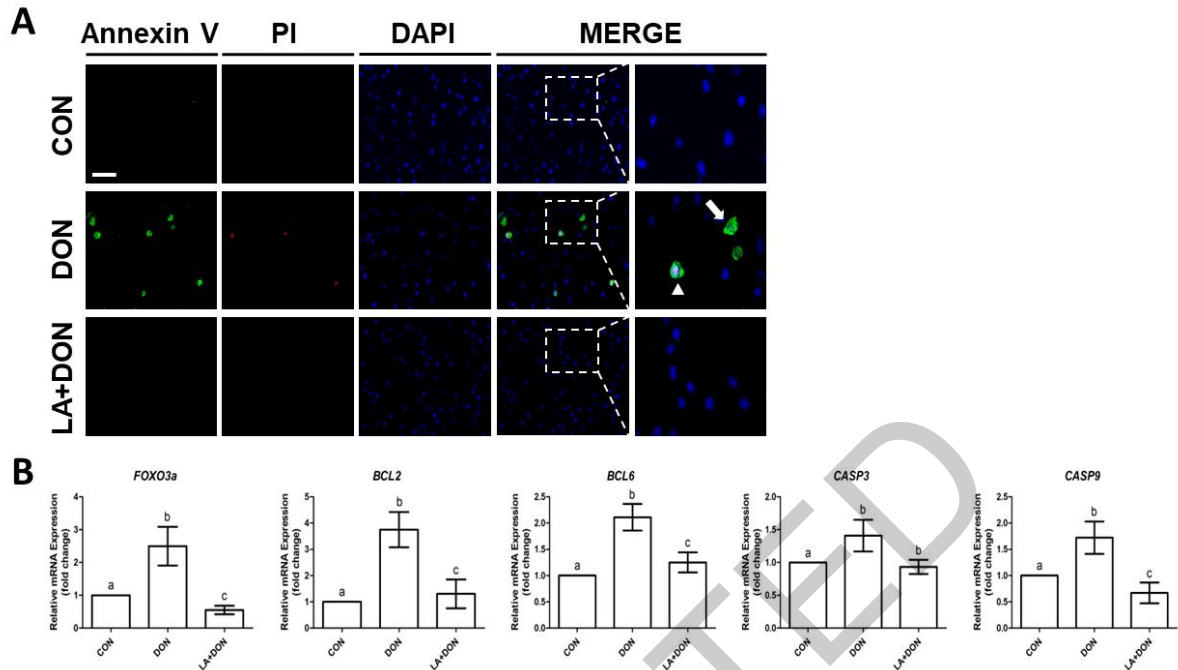


341

342 **Figure 2.** Lauric acid improves IPEC-J2 cells proliferation dysfunction by DON-induced. The WST-1
343 assay of IPEC-J2 cell treated with only DON, and DON+LA compared to untreated control for 24H
344 (n=3). Significant differences between control and treatment groups are indicated as a, b and c.

345

346

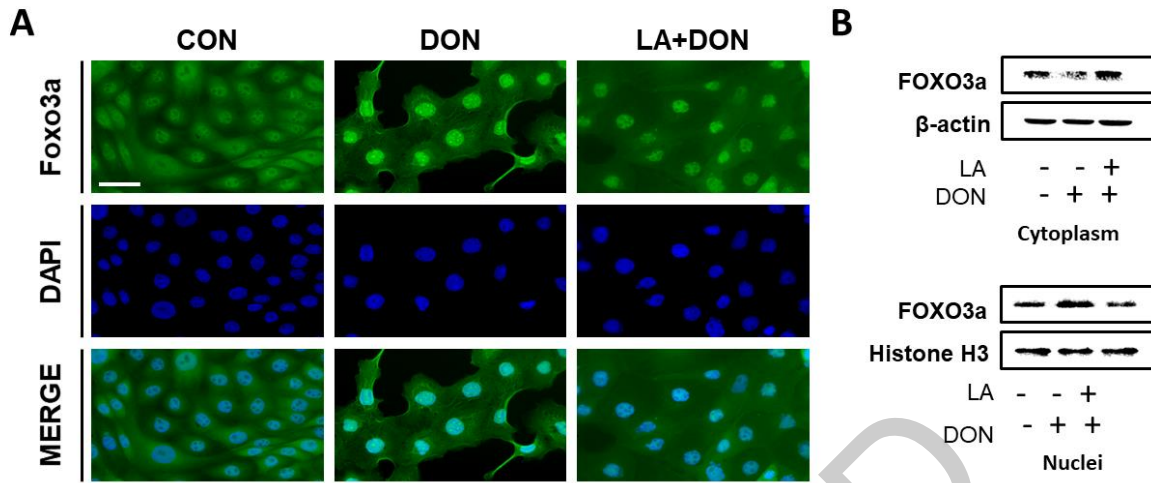


348

349 **Figure 3.** LA mitigates apoptosis and necrosis in IPEC-J2 cells. A. The apoptosis in IPEC-J2 cells
 350 treated with DON and LA+DON compared to untreated control for 48h analyzed by Annexin V staining.
 351 Apoptosis analysis was performed by single cell staining using Annexin-V (green) and propidium (red)
 352 iodide, and nuclei were stained with 4',6-diamidino-2-phenylindole (DAPI; blue). (Scale bar means 20
 353 μm). The arrow indicates that only apoptosis was induced, and the triangle indicates that both apoptosis
 354 and necrosis were induced. B. The mRNA levels of apoptosis-related genes (FOXO3a, BCL2, BCL6,
 355 CASP3, CASP9) were compared with those of the control when treated with DON alone and with DON
 356 and lauric acid (n=3). Error bars indicated standard errors (SEs) of triplicate analysis. Significant
 357 differences between control and treatment groups are indicated as a, b, c.

358

359



361

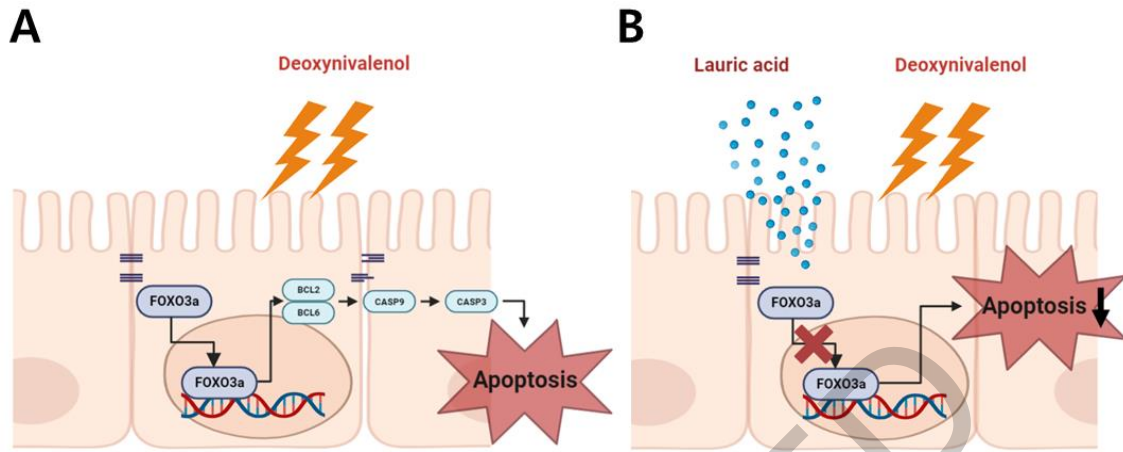
362 **Figure 4.** LA attenuates DON-induced *FOXO3a* expression and translocation. A. *FOXO3a*
 363 translocation was evaluated using immunocytochemistry. Nuclei were stained with 4',6-diamidino-2-
 364 phenylindole (DAPI; blue). (Scale bar means 40 μm). B. *FOXO3a* translocation was evaluated using
 365 Western blotting.

366

367

368

369



370

371 **Figure 5.** Schematic diagram of the current working hypothesis that LA to mitigate DON-mediated
372 apoptosis through the FOXO3a signaling pathway. A. Model illustration showing DON-induced
373 FOXO3a translocation, which induces apoptosis by regulating BCL-2 and BCL-6 expression and
374 sequentially inducing activation of CASP9 and CASP3. B. Model illustration describing that LA
375 attenuates DON-induced FOXO3a translocation, thereby reducing cell death.

376

377

379 Table 1. List of primers

Genes	Description	Accession No.		Sequence (5'-3')
GAPDH	<i>Glyceraldehyde-3-phosphate dehydrogenase</i>	NM_001206359	Forward	ACACCGAGCATCTCCTGACT
			Reverse	GACGAGGCAGGTCTCCCTAA
FOXO3	<i>Fork headbox O3</i>	NM_001135959	Forward	TCAGCCAGTCTATGCAAACC
			Reverse	CCATGAGTTCGCTACGGATA
CASP3	<i>Caspase3</i>	NM_214131	Forward	CTCAGGGAGACCTTCACAAC
			Reverse	GCACGCAAATAAACTGCTC
CASP9	<i>Caspase9</i>	XM_013998997.2	Forward	TACCCTGCCTTACCTTCCAC
			Reverse	CTGGTCTTCGGTCATCTGG
BCL-2	<i>BCL2 apoptosis regulator</i>	XM_021099593.1	Forward	AAAGCCACAAGGAGAAAAGC
			Reverse	TTCAGCCACCGTAAAATCTG
BCL-6	<i>B-cell CLL/lymphoma 6</i>	XM_005657112	Forward	GTGTCCTACGGTGCCTTTTT
			Reverse	TGACGCAGAATGTGATGAGA